HHS Public Access

Author manuscript

Proc SPIE Int Soc Opt Eng. Author manuscript; available in PMC 2017 September 20.

Published in final edited form as:

Proc SPIE Int Soc Opt Eng. 2017 February ; 10137: . doi:10.1117/12.2255640.

Automatic falx cerebri and tentorium cerebelli segmentation from Magnetic Resonance Images

Jeffrey Glaister[a], **Aaron Carass**[a,b], **Dzung L. Pham**[c], **John A. Butman**[d], and **Jerry L. Prince**[a,b]

[a]Dept. of Electrical and Computer Engineering, Johns Hopkins University, Baltimore, MD 21218, USA

[b]Dept. of Computer Science, Johns Hopkins University, Baltimore, MD 21218, USA

[c]Center for Neuroscience and Regenerative Medicine, Henry Jackson Foundation, Bethesda, MD 20817, USA

[d]Radiology and Imaging Sciences, National Institutes of Health, Bethesda, MD, 20892, USA

Abstract

The falx cerebri and tentorium cerebelli are dural structures found in the brain. Due to the roles both structures play in constraining brain motion, the falx and tentorium must be identified and included in finite element models of the head to accurately predict brain dynamics during injury events. To date there has been very little research work on automatically segmenting these two structures, which is understandable given that their 1) thin structure challenges the resolution limits of in vivo 3D imaging, and 2) contrast with respect to surrounding tissue is low in standard magnetic resonance imaging. An automatic segmentation algorithm to find the falx and tentorium which uses the results of a multi-atlas segmentation and cortical reconstruction algorithm is proposed. Gray matter labels are used to find the location of the falx and tentorium. The proposed algorithm is applied to five datasets with manual delineations. 3D visualizations of the final results are provided, and Hausdorff distance (HD) and mean surface distance (MSD) is calculated to quantify the accuracy of the proposed method. For the falx, the mean HD is 43.84 voxels and the mean MSD is 2.78 voxels, with the largest errors occurring at the frontal inferior falx boundary. For the tentorium, the mean HD is 14.50 voxels and mean MSD is 1.38 voxels.

Keywords

Magnetic resonance imaging; falx cerebri; tentorium cerebelli; segmentation

1. INTRODUCTION

The falx cerebri and tentorium cerebelli are thin dural structures found between parts of the brain.[1] The cerebrum can be divided into left and right hemispheres. The falx cerebri (or falx) is a scythe-shaped band of dura matter that separates a part of the cerebral hemispheres.

Further author information: (Send correspondence to J. Glaister) J. Glaister: jglaist1@jhu.edu.

Its inferior boundary is defined by the inferior sagittal sinus and straight sinus. The tentorium cerebelli (or tentorium) separates the cerebrum from the cerebellum and brain stem.[2] The falx and tentorium are stiffer than the brain and pia, constraining brain motion,[3] and dampening deformation across the midline.[4] Because of their stiffness and positioning with the brain, these structures affect the transfer of mechanical loads within the brain and are important in the creation of computational models of the brain for use in the study of traumatic brain injury.[5] However, the falx and tentorium are thin structures and their image contrast with respect to surrounding tissue is typically low, as shown in the T1-weighted (T1-w) magnetic resonance image (MRI) in Fig. 1(a), where the yellow arrow points to the falx and the red arrows point to the tentorium. The falx and tentorium are more apparent in other contrasts, such as gadolinium-enhanced T1-w MRI, as seen in Fig. 1(b), but those contrasts may not always be available. A 3D rendering of the falx and tentorium produced by manually delineation on a gadolinium-enhanced T1-w MRI is shown in Figs. 1(c) and (d). The cortical surface is opaque in Fig. 1(c) and translucent in Fig. 1(d) to provide context about the location of the falx and tentorium relative to other brain structures.

Recent finite element head models have incorporated the falx and tentorium in simulations.[3, 6] However, these methods used a manual or semi-automatic segmentation algorithm. Ho and Kleiven[3] delineated the falx and tentorium using tissue classification maps and anatomical atlases because the structures were not visible in their MR dataset. Chen et al.[6] manually segmented the falx from a sagittal slice of a gadolinium-enhanced MRI acquisition and estimated the location of the tentorium by fitting a 3D thin plate spline from a set of manually-selected landmarks. However, since the gadolinium-enhanced MRI are not always available, it is of interest to develop a method to segment the falx and tentorium that does not depend on the availability of that modality.

In this paper, we present a fully automatic falx and tentorium segmentation algorithm that uses a subject's T1-w MRI. Instead of finding the falx directly, we consider the gray matter (GM) labels near the falx and tentorium. We use a multi-atlas segmentation algorithm[7] to find cortical and subcortical brain structures and a cortical surface reconstruction algorithm.[8] All labels from the multi-atlas segmentation are fast marched outwards concurrently. To find the falx, we consider voxels belonging to a set of specific GM labels along the medial cortical fissue near the falx in the left cerebrum hemisphere and voxels belonging to a similar set of GM labels in the right hemisphere. The falx is generated by examining each voxel in these sets and its 26-connected neighbourhood. The tentorium is found similarly, as we examine the voxels corresponding to cerebellar GM labels inferior to the tentorium and voxels belonging to a set of cerebral GM labels superior to the tentorium.

2. METHOD

2.1 Multi-atlas Segmentation and Cortical Surface Reconstruction

An initial segmentation of the brain is determined using the algorithm by Dewey et al.[7] An intermediate brain template is created from thirty Neuromorphometrics atlases (http://www.neuromorphometrics.com). The Neuromorphemetrics atlases consist of subcortical and cortical labels, including 62 cortical labels based on gyral and sulcal landmarks. Separate labels are provided for regions on the left and right hemispheres. The subject's T1-w MR

image is registered to an intermediate template using SyN deformable registration.[9] The thirty Neuromorphemetric atlases are deformably registered to the subject in the template space to further refine the results. The label images associated with the thirty atlases are transformed into subject space. A single label map is generated from the atlases using majority voting. More sophisticated label fusion techniques are possible, but as we are only interested in the falx and tentorium, we use a fast approach that provides reasonably accurate results.

The cortical surface is reconstructed using the MACRUISE method by Huo et al.,[8] which uses the multi-atlas segmentation and the T1-w MRI acquisition. The MACRUISE algorithm ensures that the reconstructed cortical surface and multi-atlas segmentation are consistent. It does so by adjusting fuzzy membership functions for GM, white matter (WM), and cerebral spinal fluid (CSF) are using the multi-atlas segmentation. The GM membership function is also adjusted in tight sulcal regions and areas with CSF. The adjustment ensures that a gap exists between the cerebral hemisphere, which is where the falx exists. Then, a set of topology-preserving geometric deformable surface models[10] are used to reconstruct the inner, central, and outer cortical surfaces based on the adjusted membership functions. Finally, the multi-atlas segmentation is refined to be consistent with the inner and outer cortical surfaces. Fig. 2(a) shows an example of the refined multi-atlas segmentation produced by MACRUISE with an overlay of the inner and outer cortical surfaces as green and cyan contours, respectively.

2.2 Falx Segmentation

The location of the falx is estimated using expanded labels from the refined multi-atlas segmentation produced by MACRUISE. All labels in the refined multi-atlas segmentation are fast marched outwards up to 5 mm.[11] Labels are marched concurrently and stop expanding when they reach the maximum distance of 5 mm or another label. This fills the longitudinal fissure between the cerebral hemispheres with GM labels. Figure 2(a) shows the original labels, while Fig. 2(b) shows the expanded GM labels.

Of the 62 GM labels in each hemisphere, the 15 labels that lie along the medial cortical surface are used to find falx candidate voxels. A list of the labels are provided in Table 1 and was compiled by visual inspection of the segmentation results. Candidate voxels from the left cerebral hemisphere and those from the right cerebral hemisphere are considered separately. This gives us two subsets of voxels, which we denote as the *left* and *right* subsets. Figure 2(c) shows the two subsets from the expanded GM labels, with the *left* subset colored in pale yellow and the *right* subset colored in blue.

For each voxel in the *left* subset, the 26-connected neighbors are examined and if a neighbor belongs to the *right* subset, then the current voxel is classified as falx. Likewise, the voxels in the *right* subset are analyzed, and any voxels with a neighbor belonging to the *left* subset are classified as falx. Taking the union of the results from analyzing the *left* and the *right* subsets of voxels produces the final falx structure. An example of the falx at a particular coronal slice is given in Fig. 2(d).

2.3 Tentorium Segmentation

The location of the tentorium is defined in a similar manner as the falx. Seven GM labels from the inferior cerebral cortex that are superior to the tentorium as listed in Table 2 are chosen. The subset of voxels belonging to these labels is denoted as the *cerebrum* subset. All the cerebellum GM labels are chosen and this subset of voxels is denoted as the *cerebellum* subset. An example of the tentorium candidate voxels is shown in Fig. 3(b). Each voxel in the *cerebrum* subset with a neighbor in the *cerebellum* subset are classified as belonging to the tentorium class and likewise for each voxel in the *cerebellum* subset with a neighbor in the *cerebrum* subset. The final tentorium is produced by taking the union of the results from analyzing each of the subsets. An example of the final tentorium is shown in Fig. 3(c).

3. EXPERIMENTS AND RESULTS

The proposed method is applied to five subjects that have T1-w magnetization prepared rapid gradient echo (MPRAGE) images. The five subjects also had MPRAGE with gadolinium contrast, which were only used to produce manual delineations because of the improved contrast between the falx and tentorium and surrounding tissue. All data was acquired on a Siemens Biograph mMR 3T imaging platform. The five patients' T1-w MRI first underwent standard neuroimaging preprocessing, which includes inhomogeneity correction,[12] skull stripping,[13] and affine registration to an MNI atlas at 0.8 mm isotropic resolution. To quantify the performance of our proposed method, we use two metrics that measure surface distance between the automatic result and manual delineation: Hausdorff distance (HD)[14] and mean surface distance (MSD). HD finds the maximum of the minimum distances between two surfaces. To calculate the MSD, we find the minimum distance at each voxel on one surface to the nearest voxel on the other surface and take the average across all voxels on both surfaces. HD and MSD are reported in voxels.

The manual delineations were generated using a protocol similar to that specified by Chen et al.,[6] which uses the gadolinium-enhanced T1-w MRI. For the tentorium, a set of points on the tentorium were identified in coronal slices of the gadolinium-enhanced T1-w MRI. A surface in the shape of the tentorium was fit based on the manually selected points using a smoothing spline algorithm and the the gadolinium-enhanced T1-w MRI intensities on the surface were interpolated using trilinear interpolation. The final tentorium was manually segmented on this surface using these intensities. The same procedure was used for the falx, except that the rater identified points on the falx in the gadolinium-enhanced T1-w MRI.

Figure 4 shows a 3D rendering of both the manually delineated falx and tentorium (with and without the cortical surface overlaid) and the automatic result for three subjects. The color of the rendering in the automatic result shows the distance to the nearest point on the manually delineated surface, in voxels. Qualitatively, there appears to be two areas where the proposed algorithm fails to properly find the falx. The largest area of disagreement occurs in the frontal inferior falx, where the proposed algorithm generates a falx that curves around the corpus callosum. The proposed algorithm also misplaces the rest of the inferior falx by placing inferior boundary too low in the limbic cortex. Both of these errors are a result of the proposed algorithm relying on Neuromorphemetric labels, particularly the frontal lobe and limbic cortex labels. The boundaries of these labels do not align with that of the falx as the

falx is only partially contained in those labels. The other subjects that are not shown exhibited the same errors. The largest surface distances in the tentorium occur at the lateral edges, but are small relative to errors in the falx. This is reflected in the HD and MSD for the five subjects, which are provided in Table 3. The HD and MSD is much higher for the falx compared to the tentorium for all five subjects.

4. CONCLUSION

In this work, we present an automatic method to segment the falx cerebri and tentorium cerebelli. The proposed method uses the results of a multi-atlas segmentation and cortical reconstruction algorithm. After expanding GM labels using fast marching, neighbors of certain GM labels are used to determine if a voxel belongs to the falx or tentorium. The proposed algorithm is applied to five datasets with manual delineations generated using contrast-enhanced T1-w MRI. Quantitatively, the tentorium produced by the proposed method has a mean HD of 14.50 voxels and mean MSD of 1.38 voxels, while the falx has a mean HD of 43.84 voxels and mean MSD of 2.78 voxels. The high HD and MSD in the falx is caused by brain labels in the frontal lobe and limbic cortex that only partially contain the falx. This is confirmed by 3D visualizations that show that large errors occur in the frontal inferior falx, while small errors occur at the lateral edges of the tentorium. Future work will add image features from different MR modalities to improve segmentation and refine the falx boundaries.

Acknowledgments

This project is funded by the NIH/NINDS through grant R01NS055951. Jeffrey Glaister is funded by the National Science and Engineering Research Council of Canada.

References

1. Bandak, FA. Biomechanics of impact traumatic brain injury. In: Ambrósio, JAC.Pereira, MFOS., da Silva, FP., editors. Crashworthiness of Transportation Systems: Structural Impact and Occupant Protection. Springer; 1997. p. 53-93.
2. Voo L, Kumaresan S, Pintar FA, Yoganandan N, Sances A. Finite-element models of the human head. Medical and Biological Engineering and Computing. 1996; 34(5):375–381. [PubMed: 8945864]
3. Ho J, Kleiven S. Can sulci protect the brain from traumatic injury? Journal of Biomechanics. 2009; 42(13):2074–2080. [PubMed: 19679308]
4. Miga, MI., Paulsen, KD., Kennedy, FE., Hartov, A., Roberts, DW. Model-updated image-guided neurosurgery using the finite element method: Incorporation of the falx cerebri. In: Taylor, C., Colchester, A., editors. Medical Image Computing and Computer-Assisted Intervention – MICCAI'99; Second International Conference; Cambridge, UK. September 19–22, 1999; Berlin, Heidelberg: Springer Berlin Heidelberg; 1999. p. 900-909.Proceedings
5. Yoganandan, N., Li, J., Zhang, J., Pintar, FA. Role of Falx on Brain Stress-Strain Responses. Springer; Netherlands, Dordrecht: 2009. p. 281-297.
6. Chen I, Coffey AM, Ding S, Dumpuri P, Dawant BM, Thompson RC, Miga MI. Intraoperative brain shift compensation: Accounting for dural septa. IEEE Trans Biomed Eng. Mar.2011 58:499–508. [PubMed: 21097376]
7. Dewey, BE., Carass, A., Blitz, AM., Prince, JL. Efficient multi-atlas registration using an intermediate template image. Proceedings of SPIE Medical Imaging (SPIE-MI 2017); Orlando, FL. February 11–16, 2017; 2017.

8. Huo Y, Plassard AJ, Carass A, Resnick SM, Pham DL, Prince JL, Landman BA. Consistent cortical reconstruction and multi-atlas brain segmentation. NeuroImage. 2016; 138:197–210. [PubMed: 27184203]
9. Avants BB, Epstein CL, Grossman M, Gee JC. Symmetric diffeomorphic image registration with cross-correlation: Evaluating automated labeling of elderly and neurodegenerative brain. Medical Image Analysis. 2008; 12(1):26–41. Special Issue on The Third International Workshop on Biomedical Image Registration WBIR 2006. [PubMed: 17659998]
10. Han X, Xu C, Braga-Neto U, Prince JL. Topology correction in brain cortex segmentation using a multiscale, graph-based algorithm. IEEE Transactions on Medical Imaging. Feb.2002 21:109–121. [PubMed: 11929099]
11. Sethian JA. Fast marching methods. SIAM Review. 1999; 41(2):199–235.
12. Tustison NJ, Avants BB, Cook PA, Zheng Y, Egan A, Yushkevich PA, Gee JC. N4ITK: Improved N3 Bias Correction. IEEE Trans Med Imag. Jun.2010 29:1310–1320.
13. Roy S, Butman JA, Pham DL. Robust skull stripping using multiple MR image contrasts insensitive to pathology. NeuroImage. 2017; 146:132–147. [PubMed: 27864083]
14. Huttenlocher DP, Klanderman GA, Rucklidge WJ. Comparing images using the Hausdorff distance. IEEE Transactions on Pattern Analysis and Machine Intelligence. Sep.1993 15:850–863.

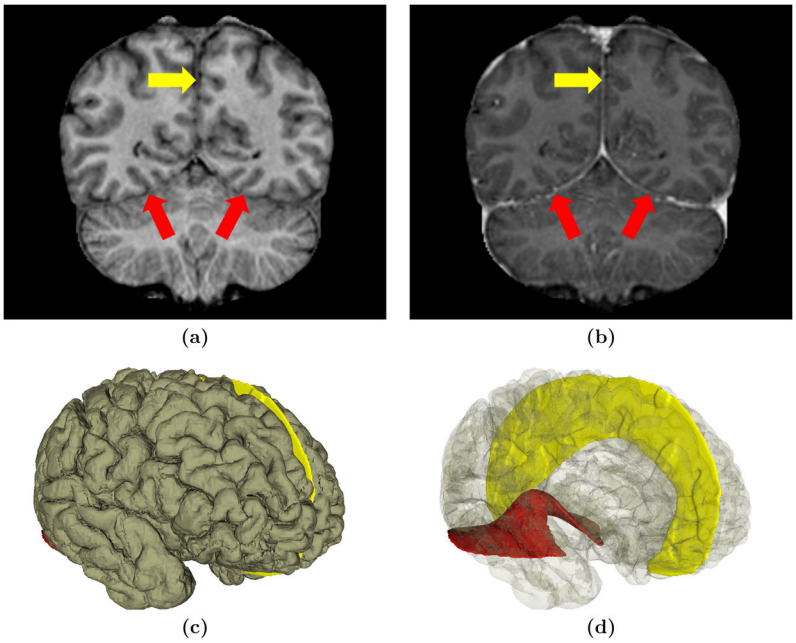

Figure 1.

Coronal slice of a T1-weighted MR image showing the falx (yellow arrow) and tentorium (red arrow) in **(a)**, the same coronal slice in a gadolinium-enhanced T1-w MRI showing the falx (yellow arrow) and tentorium (red arrow) in **(b)**, and a 3D rendering of the falx (yellow) and tentorium (red), with the outer cortical surface overlaid in **(c)** and translucent in **(d)**.

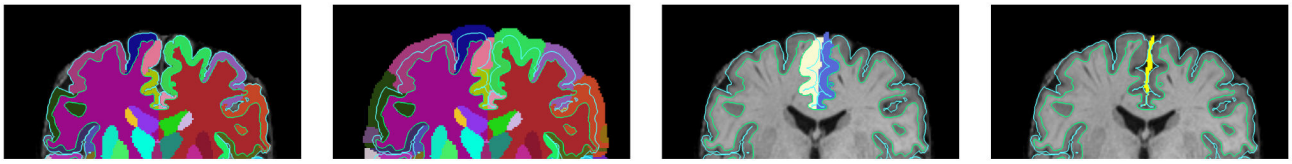

Figure 2.

Coronal view of the steps in the proposed falx segmentation method: **(a)** the refined multi-atlas segmentation; **(b)** the extended segmentation labels; **(c)** the falx candidate voxels—those voxels on the border between the *left* subset (blue) and the *right* subset (pale yellow); and **(d)** the final falx segmentation, shown in yellow. The inner and outer cortical surfaces are overlaid, in each view, as green and cyan contours respectively.

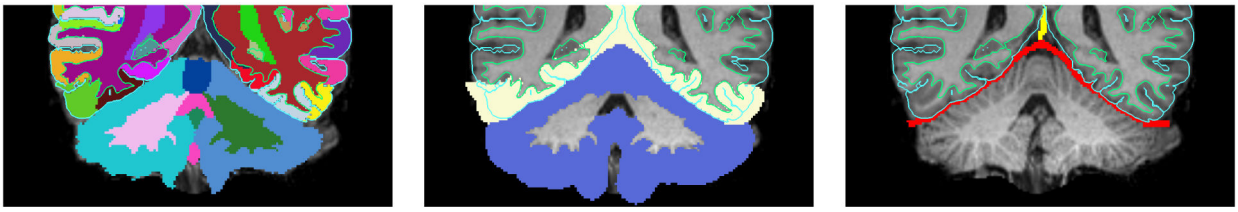

Figure 3.

Coronal view of the steps in the proposed tentorium segmentation method: **(a)** the refined multi-atlas segmentation; **(b)** the tentorium candidate voxels—those voxels on the border between the *cerebellum* subset (blue) and the *cerebrum* subset (pale yellow); and **(c)** the final tentorium segmentation, shown in red. The inner and outer cortical surfaces are overlaid, in each view, as green and cyan contours respectively.

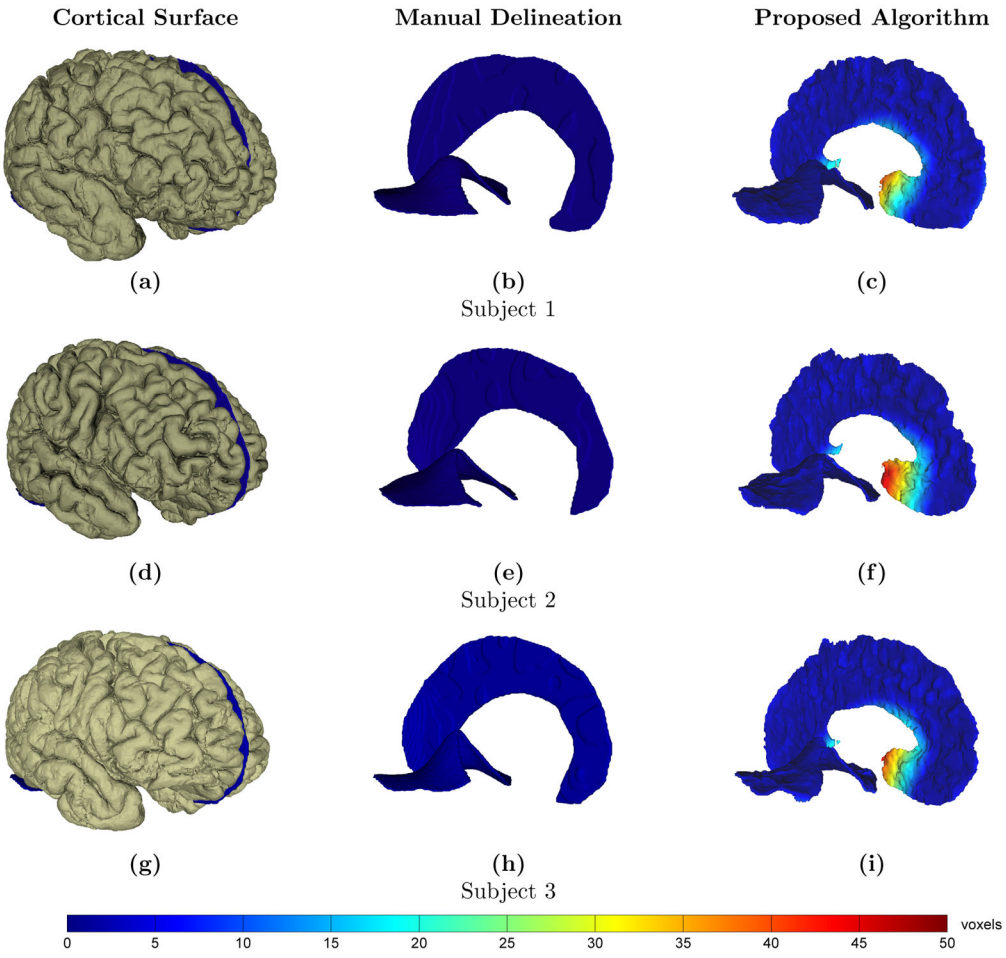

Figure 4.

3D renderings of the cortical surface (**(a)**, **(d)**, and **(g)**) and the falx and tentorium produced by manual delineation (**(b)**, **(e)**, and **(h)**) and by the proposed algorithm (**(c)**, **(f)**, and **(i)**) for three subjects. The color of the surface indicates the minimum distance from that point on the falx or tentorium surface to the surface of the corresponding structure in the manual delineation, in voxels.

Table 1

Neuromorphemetrics atlas GM labels used to find the falx.

Lobe	Label
Frontal Lobe	Frontal pole, gyrus rectus, subcallosal area, medial frontal cortex, precentral gyrus (medial segment), superior frontal gyrus (medial segment), supplementary motor cortex
Parietal Lobe	Postcentral gyrus (medial segment), precuneus
Occipital Lobe	Calcarine cortex, cuneus, lingual gyrus
Limbic Cortex	Anterior cingulate gyrus, middle cingulate gyrus, posterior cingulate gyrus

Table 2

Neuromorphemetrics atlas GM labels used to find the tentorium.

Lobe	Label
Occipital Lobe	Inferior occipital gyrus, lingual gyrus, occipital fusiform gyrus
Temporal Lobe	Fusiform gyrus, inferior temporal gyrus,
Limbic Cortex	Posterior cingulate gyrus, parahippocampal gyrus

Table 3

HD and MSD Results

Subject	Falx cerebri		Tentorium cerebelli	
	HD (voxels)	MSD (voxels)	HD (voxels)	MSD (voxels)
1	40.31	2.52	15.65	1.19
2	49.25	2.98	19.75	1.40
3	43.57	2.49	8.78	1.30
4	44.64	3.36	11.75	1.57
5	41.41	2.55	16.55	1.42
Mean	43.84	2.78	14.50	1.38
Standard Deviation	3.48	0.38	4.28	0.14